IRSTI 29.19.22 https://doi.org/10.26577/phst20251216

In-situ raman analysis of carbon nanowalls during electrochemical measurement

R.Ye. Zhumadilov[1,2,3*], B.Ye. Zhumadilov[1,2], R.R. Nemkayeva[1,2], H. Kondo[4], A.A. Markhabayeva[1,2], Y. Yerlanuly[1,2,3*], M.T. Gabdullin[1,2,3] and M. Hori[5]

[1]Kazakh-British Technical University, Almaty, Kazakhstan
[2]Al-Farabi Kazakh National University, Almaty, Kazakhstan
[3]Institute of Applied Science and Information Technologies, Almaty, Kazakhstan
[4]Kyushu University, Fukuoka, Japan
[5]Center for Low-temperature Plasma Sciences, Nagoya University, Nagoya, Japan
*e-mail: rakimzhan@gmail.com, yerlanuly@physics.kz
(Received February 27, 2025; received in revised form May 12, 2025; accepted May 28, 2025)

This study focuses on the synthesis of carbon nanowalls (CNWs) and nitrogen-doped CNWs using the RI-PECVD method and their investigation through in situ Raman spectroscopy during voltammetric cycling and potentiostatic charging under both reduction and oxidation potentials. CNWs were synthesized on Ti/SiO_2/Si substrates. Electrochemical experiments were conducted in a three-electrode cell with CNWs as the working electrode, and analytes such as urea, citric acid, and hydrogen peroxide (H_2O_2) were used to study their effects during in situ Raman measurements. The Raman spectra of CNWs and N-doped CNWs were recorded in a voltage range of -1 V to 1 V (vs. Ag/AgCl), revealing no significant shifts in peak positions but showing an increase in the G to 2D peak ratio at higher voltages, indicating strong electron doping. The cyclic voltammetry results demonstrated that nitrogen doping enhances the reductive current of CNWs, with a clear reduction peak observed at -0.7 V across all analytes. The ID/IG peak ratio of N-doped CNWs increased upon analyte addition, suggesting the introduction of defects and restoration of sp2 domains. Furthermore, the position of the G and 2D peaks shifted significantly in response to different analytes. Sharper fluctuations were observed in N-doped CNWs. These results not only provide valuable insights into the electrochemical properties of CNWs but also highlight their potential for electrochemical sensing applications, offering a promising avenue for future research and development in this field.

Key words: carbon nanowalls, in situ raman, nitrogen doping, electrochemical reduction.
PACS number(s): 61.46.−w.

1 Introduction

Raman spectroscopy, particularly in its in situ form, plays a crucial role in the study of electrochemical reactions. This technique, which is the preferred method for characterizing graphene and other carbon-based materials due to its non-destructive nature, provides real-time insights into several important areas, including interfacial phenomena, doping, interlayer coupling, structural defects, and chemical functionalization [1]. In-situ Raman spectroscopy is particularly valuable as it enables the real-time visualization and monitoring of electrochemical reactions [2–8]. The emergence of vibrational bands, which correspond to the presence of specific bonds or compounds, under applied potentials can reveal the reasons behind improved electrocatalytic performance [9]. Additionally, peak position shifts often indicate chemical composition changes resulting from chemical interactions, providing critical information about reaction mechanisms. This feature is fundamentally significant because certain chemical changes related to the reaction mechanism occur exclusively during the reaction itself and are reversed afterward. Changes detected through ex-situ techniques may not appear in in-situ characterization measurements and could, therefore, be entirely unrelated to the actual reaction [10]. Such spectroscopic data can be used

to gather diverse information about electrochemical reactions, including the structural transitions of electrocatalysts, interfacial species on surfaces, and localized species in the electrolyte within the electrical double layer (EDL) region [1]. During the electrochemical process, electrodes coated with active materials are exposed to harsh chemical and electrochemical conditions. Consequently, many materials are unable to preserve their structure under these operating conditions. Structural changes frequently take place either just before or at the early stages of electrocatalysis. Structural changes are commonly caused by redox reactions, where electrochemical reduction or oxidation leads to the transformation of electrocatalysts into species with varying oxidation states. Additionally, phase transitions occur when a chemically unstable phase converts to a stable one, and decomposition happens when electrochemically unstable materials with weak internal bonds break down [2, 11–13].

The integration of Raman spectroscopy with electrochemistry, known as Raman spectroelectrochemistry, has already demonstrated its effectiveness in investigating graphene, fullerenes, and carbon nanotubes [14]. In graphene's Raman spectra, the G and 2D modes, symmetry allowed features, are of particular interest [15, 16]. While these modes are also observed in Raman spectra of graphene-derived materials, their specific Raman shifts, line widths, and intensities are influenced by factors such as laser excitation energy, the number of graphene layers, doping levels, and strain [17, 18]. Additionally, the D peak may appear in the Raman spectra of certain graphene samples, indicating the presence of symmetry disrupting perturbations. Recent research has explored the spectroelectrochemical behavior of the D band, highlighting its tunability in response to applied potential, both reversibly and irreversibly [12, 19]. In recent years, the electrochemical properties of graphene-based nanomaterials have been studied in detail using in-situ Raman spectroscopy. For example, Milan Bouša et al. investigated graphene oxide and graphene nanoplatelets with in-situ spectroelectrochemistry during voltammetric cycling and potentiostatic charging at both reductive and mildly oxidative potentials [12]. Minkyung Choi et al. conducted in-situ Raman measurements of a graphene microbridge on SiO_2/Si substrates in air at a current density of up to 2.58×10^8 A/cm^2 [20]. Additionally, in a study by Binder et al., the authors induced hydrogen chemisorption on a bilayer graphene sample by intentionally applying a high gate voltage. The chemisorption process was investigated using in-situ Raman spectroscopy, observing the emergence of Si-H and C-H modes and an increase in the intensity of the D-band. This process was partially reversible when negative gate voltages were applied. Thus, by varying the gate voltage, the authors achieved an electrical switch for hydrogen chemisorption on graphene [21]. However, despite these advancements, there is no information in the literature on the study of the electrochemical properties of CNWs using in-situ Raman spectroscopy. In addition, due to high specific area and peculiar morphology, CNWs are expected to react on external changes (electrolyte media and potential) noticeably strongly.

Carbon nanowalls (CNWs) are a form of carbon allotrope composed of three-dimensional networks of vertically aligned graphene sheets [22]. They are attracting increasing interest as a novel material for electrochemical sensing devices due to their high electrical and thermal conductivity, excellent electrocatalytic activity, large surface area, and high sensitivity to various analytes. The free bonds at the edges of the vertically aligned graphene sheets make CNWs a promising electrode material for electrochemical probing [23–29]. Despite their unique behavior as electrode materials, the mechanisms behind many of their specific properties are still not fully understood. The impact of different analytes such as urea, hydrogen peroxide (H_2O_2), and citric acid on the electrochemical properties of CNWs can be thoroughly examined using in-situ Raman spectroscopy. Urea is a key biomarker in medical diagnostics, particularly for kidney function monitoring, while hydrogen peroxide is widely used as an indicator of oxidative stress and plays a critical role in biochemical and environmental processes. Citric acid, on the other hand, is an important organic acid involved in metabolic pathways and is commonly found in food and pharmaceutical industries.

Thus, the work focuses on the synthesis of CNWs and nitrogen-doped CNWs, which are synthesized using the RI-PECVD method. The CNWs were investigated using in situ Raman spectroscopy during voltammetric cycling, a process involving the measurement of Raman spectra of the CNWs at different electrochemical potentials, as well as potentiostatic charging at both reducing and oxidizing potentials. This investigation provides insights into the changes in the structure and properties of CNWs under different electrochemical conditions.

2 Materials and methods

2.1 Methods

The synthesis of CNWs films is carried out using the RI-PECVD method. The experimental setup,

synthesis processes are described in detail in previous work [26, 30]. CNWs were synthesized on Ti\SiO_2\Si substrates (4 × 4 cm² in size), with both Ti and SiO_2 layers having a thickness of 200 nm. A gas mixture of CH_4 (100 sccm) and H_2 (50 sccm) was introduced into the chamber for growth without nitrogen addition, while for nitrogen-assisted growth, 20 sccm of N_2 was also introduced. The total gas pressure was maintained at 3 Pa. Both the surface-wave plasma (SWP) microwave source and the capacitively coupled plasma (CCP) very high frequency (VHF) source operated at 400 W. During the CNW growth, the substrate heater temperature was consistently maintained at 800 °C. All in-situ electrochemical experiments were conducted using a three-electrode electrochemical cell with a 30 mL volume (Dek Research) [31–33], where the CNWs film served as the working electrode, as illustrated in Figure 1. A Pt wire was used as counter electrode, while a Ag/AgCl (3 M KCl, E° = 0.197 V) electrode was used as reference electrode. The 0.1 M phosphate buffer solution (PBS (pH 7.2, Sigma Aldrich)) was used as supporting electrolyte. The Metrohm potentiostat (μStat-i 400) was used to perform the electrochemical measurements. Urea (98%), citric acid (99%) and hydrogen peroxide (30%), purchased from Sigma-Aldrich, were used as analytes to investigate the electrochemical reaction during in-situ Raman measurements.

The Raman spectra were recorded by Raman spectrometer (NT-MDT Solver Spectrum). A 473 nm diode laser was focused on the surface of the CNWs films utilizing a 50× long working distance microscope objective. The laser power was maintained at 0.7 mW and exposure time was set to 60 seconds.

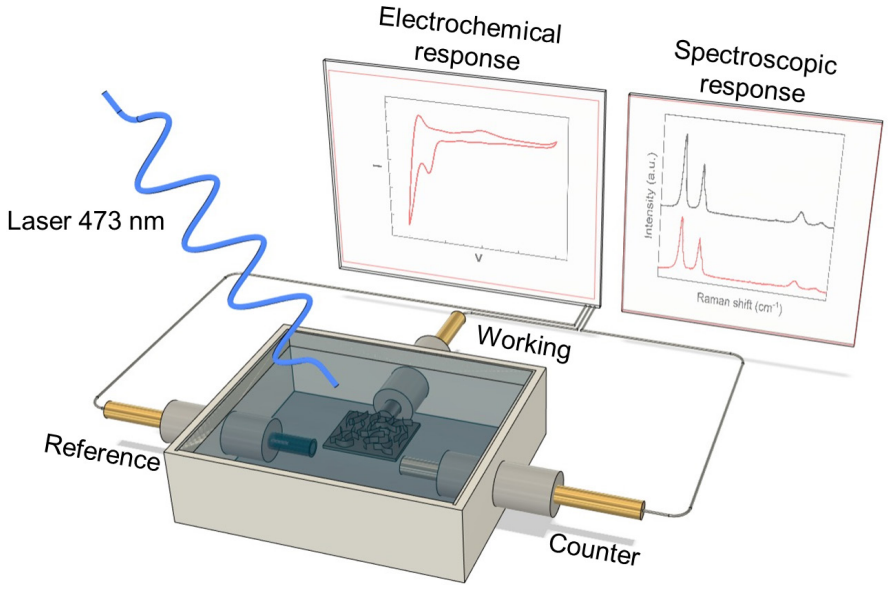

Figure 1 – Schematic illustration of in-situ Raman spectroscopy system.

3 Results and discussion

Figure 2 shows the Raman spectra of CNWs films synthesized at 0 and 20 sccm nitrogen flow rates. Typical D, G, D′, G′ (2D), and G + D peaks are observed in the CNWs Raman spectra [34]. The D peak is characteristic of samples with defects in sp^2-structures. The presence of the G peak indicates the synthesis of graphitized carbon. The D′ shoulder peak arises from edges as well as lattice defects in the graphene structure and indicates disorder in the final dimensions of the sp^2 crystal. The appearance of the G′ peak indicates long-range order in the structure [35, 36].

Figure 3 presents the Raman spectra for (a) CNWs and (b) N-doped CNWs, recorded over a potential range of -1 V to 1 V (vs. Ag/AgCl) in 0.2 V increments during electrochemical measurements in PBS. The voltage range of -1 to 1 V was selected, as further increases in both negative and positive voltages result in material degradation and detachment from the substrate. Analysis indicates no significant effect on the peak positions with increased voltage. Moreover, the analysis of the D to G peak intensity

ratio demonstrated minimal variation, whereas the G to 2D peak ratio exhibited an increase at higher voltages of +1 V (see Figure S1). This behaviour is indicative of strong electron doping [37–39]. Doping will increase the number of charge carriers, thereby increasing the probability of a scattering event. Consequently, the 2D peak intensity should decrease [2, 3, 40].

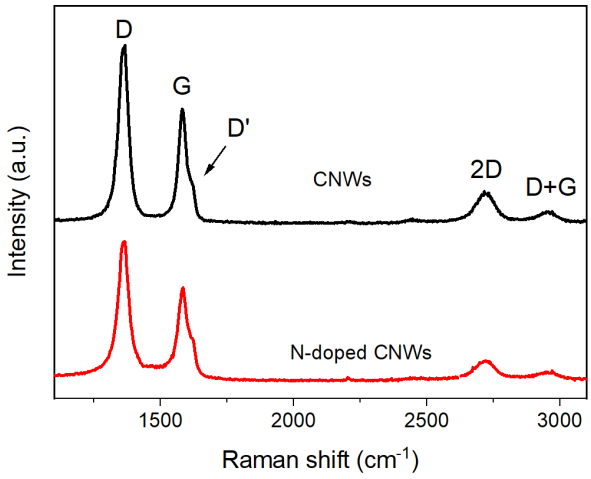

Figure 2 – Raman spectroscopy analysis of the CNWs films synthesized at 0 and 20sccm nitrogen flow rate.

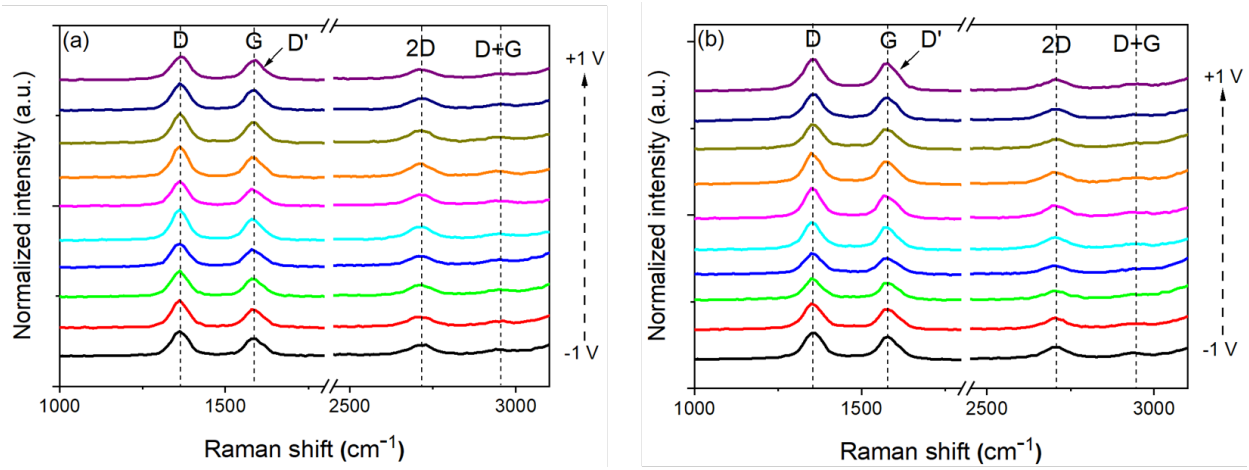

Figure 3 – Raman spectra of (a) CNWs and (b) N-doped CNWs, recorded in the potential range from -1 V to 1 V (vs. Ag/AgCl) with a step of 0.2 V in the PBS electrolyte.

The electrochemical characteristics of CNW films were assessed using a three-electrode setup with 0.1 M PBS solution serving as the electrolyte. Figure 4 shows the cyclic voltammetry (CV) of CNWs, and N-doped CNWs between -1 V and 1 V (vs. Ag/AgCl) at a scan rate of 20 mV/s in the (a) bare PBS solution, and in the presence of 5 mM (b) urea, (c) H_2O_2, (d) citric acid. As the potential is swept in a cyclic voltammogram, a peak current is produced within a certain potential range where the working electrode interacts with the substance, indicating the occurrence of the reaction. It is notable from Figure 4 that reductive current significantly increases in the case of N-doped CNWs (after nitrogen doping of CNWs). A clear reduction peak can be observed for CNWs and N-doped CNWs in all studied analytes at -0.7 V versus Ag/AgCl.

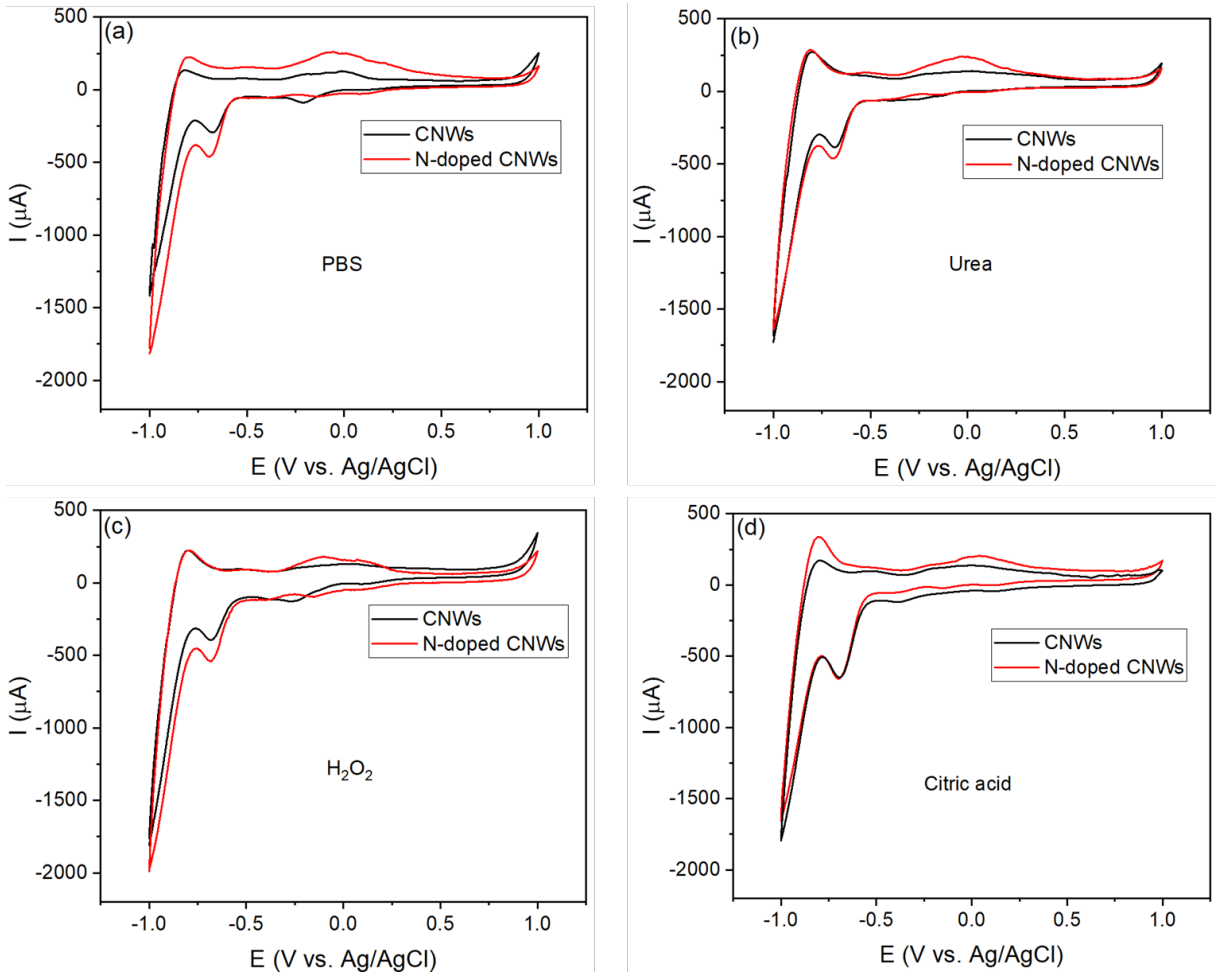

Figure 4 – Cyclic voltammograms obtained using undoped CNWs (a), and N-doped CNWs (b) in the PBS solution, and in the presence of 5 mM urea, H_2O_2, citric acid.

Figure 5a shows the ratio of ID/IG peak when 5mM of different analytes were added to the surface of the CNWs and N-doped CNWs films. The ID/IG peak ratio of the CNWs remains unchanged upon the addition of analytes. In contrast, for N-doped CNWs, the initial ID/IG ratio is 1.4 and increases to 1.6 upon the addition of analytes such as H_2O_2, citric acid, and urea. An increase in the ID/IG ratio suggests the restoration of sp^2 domains caused by the introduction of defects of various types (e.g., vacancies, functionalization) [41–43]. The observed changes might be attributed to the intercalation of H+ ions from acidic electrolytes or the incorporation of water molecules into the CNWs film. These processes can cause distortions in the periodic lattice structure of CNWs [41].

Figure 5b shows the ratio of the ID/IG peaks of CNWs in PBS solution and in different analytes at applied -0.7 V negative potential to the CNWs film. The analysis indicates that applying a negative potential has no significant effect on the ID/IG peak ratio, demonstrating the structural stability of the CNWs. The specifics of the Raman spectra analysis of the CNWs films can be found in the Supporting Information (see Figure S2).

Summarizing, the addition of analytes such as urea, H_2O_2, and citric acid to the surface of CNWs results in the formation of a defective material (without applying an external potential). To gain deeper insights into the mechanism of electrochemical reduction of CNWs, a constant potential of -0.7 V was applied to the electrodes in a PBS solution with the addition of various analytes, and the resulting electrodes were characterized using Raman spectroscopy (Fig. 5). As shown, regardless of the type of analyte, the electrochemically reduced CNWs exhibited minimal modification of structural parameters (with the ID/IG ratio remaining nearly unchanged). This may be attributed to the lower efficiency of O-group removal, leading to a reduced number of defects [44, 45].

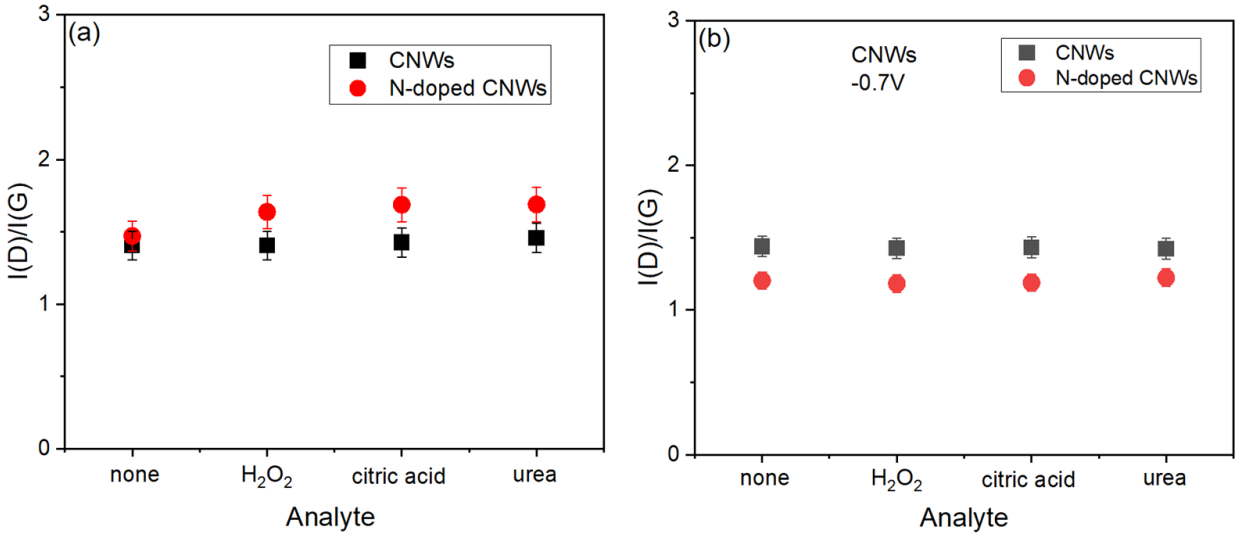

Figure 5 – (a) Ratio of the ID/IG peaks of CNWs when 0.5 mM of different analytes were added to the surface of the CNWs film. (b) Ratio of the ID/IG peaks of CNWs in PBS solution and in different analytes at applied -0.7 V negative potential to the CNWs film.

Figure 6(a) and (b) clearly demonstrates the effect of different analytes on the position of the G and 2D peaks, respectively. The positions of the G and 2D peaks are changed by +2 and +3 cm^{-1}, respectively, upon addition of analytes. The fluctuations in the Raman spectra of N-doped CNWs are much sharper, with the position of the G and 2D peaks changing by +4 and +9 cm^{-1}, respectively, upon addition of analytes. The G and 2D band shifts are governed by mild oxidation/reduction and/or by charging-induced lattice expansion and lattice contraction upon addition of different analytes. The blue shift observed in the Raman bands, moving to higher wavenumbers, is attributed to the growing structural disorder resulting from the presence of oxygen-containing functional groups attached to the graphene sheets. These imperfections stem from intrinsic defects introduced by the attachment of oxygen functional groups to the plane and edges of graphene sheets [46–49].

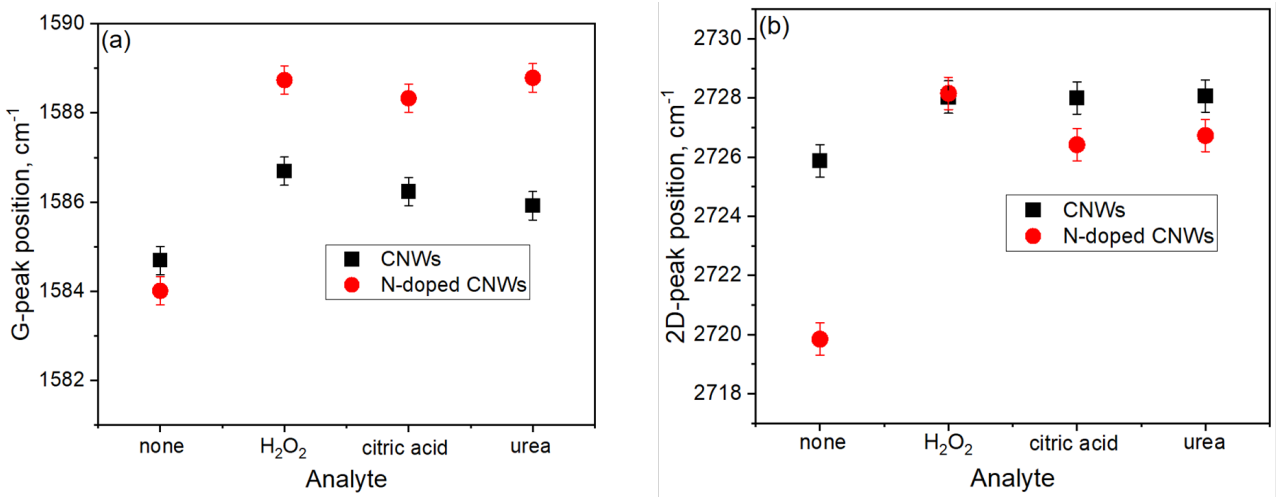

Figure 6 – The G-peak (a), and 2D-peak (b) position extracted from the in-situ Raman spectrum vs different analytes.

4 Conclusions

In conclusion, this study comprehensively investigated the structural and electrochemical properties of CNWs and N-doped CNWs through Raman spectroscopy and cyclic voltammetry under varying conditions. The introduction of analytes such as urea, H_2O_2, and citric acid led to noticeable changes in the structural parameters of the CNWs, with the ID/IG ratio increasing in N-doped CNWs, indicating defect formation and restoration of sp^2 domains. Electrochemical measurements demonstrated that applying a constant potential of -0.7 V in the presence of analytes minimally affected the structural integrity of the CNWs, as evidenced by the stable ID/IG ratio. However, N-doped CNWs exhibited sharper fluctuations in the positions of the G and 2D peaks, reflecting their enhanced sensitivity to analytes and structural changes due to oxidation/reduction processes. The observed blue shifts in Raman bands were attributed to structural disorder induced by oxygen functional groups.

Overall, the results highlight the structural stability and tunable properties of CNWs and N-doped CNWs, making them promising materials for applications requiring robust electrochemical performance and analyte sensitivity. Further studies focusing on the mechanisms of defect formation and reduction processes could provide deeper insights into optimizing their functionality for specific applications.

Acknowledgments. MTG thanks the Scientific Research Grant (grant number: AP23484100) from the Committee of Science of the Ministry of Science and Higher Education of the Republic of Kazakhstan.

References

1. Zheng W. Beginner's Guide to Raman spectroelectrochemistry for electrocatalysis study // Chemistry–Methods. – 2023. – Vol. 3. – Art. e202200042. https://doi.org/10.1002/cmtd.202200042

2. Parpal M., El Sachat A., Sotomayor Torres C.M., Gómez-Romero P., Rueda-García D., Chavez-Angel E. In situ Raman analysis of reduced-graphene oxide-based electroactive nanofluids // Diam Relat Mater. – 2024. – Vol. 141. – Art. 110541. https://doi.org/10.1016/j.diamond.2023.110541

3. Yadav R., Joshi P., Hara M., Yoshimura M. *In situ* electrochemical Raman investigation of charge storage in rGO and N-doped rGO // Physical Chemistry Chemical Physics. – 2021. – Vol. 23. – P. 11789–11796. https://doi.org/10.1039/D1CP00248A

4. Deng Y., Yeo B.S. Characterization of electrocatalytic water splitting and CO_2 reduction reactions using in situ/operando Raman spectroscopy // ACS Catal. – 2017. – Vol. 7. – P. 7873–7889. https://doi.org/10.1021/acscatal.7b02561

5. Liu S., Zhang G., Feng K., Han Y., He T., You J., Wu Y. *In Situ* Raman spectroscopy studies on $La_2 CaB_{10}O_{19}$ crystal growth // Cryst Growth Des. – 2020. – Vol. 20. – P. 6604–6609. https://doi.org/10.1021/acs.cgd.0c00761

6. Zhu H., Yu G., Guo Q., Wang X. In situ Raman spectroscopy study on catalytic pyrolysis of a bituminous coal // Energy & Fuels. – 2017. Vol. 31. – P. 5817–5827. https://doi.org/10.1021/acs.energyfuels.6b03042

7. Wu H.-L., Huff L.A., Gewirth A.A. In situ Raman spectroscopy of sulfur speciation in lithium–sulfur batteries // ACS Appl Mater Interfaces. – 2015. – Vol. 7. – P. 1709–1719. https://doi.org/10.1021/am5072942

8. Ou J.Z., Campbell J.L., Yao D., Wlodarski W., Kalantar-zadeh K. In situ Raman spectroscopy of H_2 gas interaction with layered MoO_3 // The Journal of Physical Chemistry C. – 2011. – Vol. 115. – P. 10757–10763. https://doi.org/10.1021/jp202123a

9. Wain A.J., O'Connell M.A. Advances in surface-enhanced vibrational spectroscopy at electrochemical interfaces // Adv Phys X. – 2017. – Vol. 2. – P. 188–209. https://doi.org/10.1080/23746149.2016.1268931

10. Yoo R.M.S., Yesudoss D., Johnson D., Djire A. A Review on the application of In-situ Raman spectroelectrochemistry to understand the mechanisms of hydrogen evolution reaction // ACS Catal. – 2023. Vol. 13. – P. 10570–10601. https://doi.org/10.1021/acscatal.3c01687

11. van den Beld W.T.E., Odijk M., Vervuurt R.H.J., Weber J.-W., Bol A.A., van den Berg A., Eijkel J.C.T. In-situ Raman spectroscopy to elucidate the influence of adsorption in graphene electrochemistry // Sci Rep. – 2017. – Vol. 7. – Art. 45080. https://doi.org/10.1038/srep45080

12. Bouša M., Frank O., Jirka I., Kavan L. *In situ* Raman spectroelectrochemistry of graphene oxide // physica status solidi (b). – 2013. – Vol. 250. – P. 2662–2667. https://doi.org/10.1002/pssb.201300105

13. Frank O., Dresselhaus M.S., Kalbac M. Raman spectroscopy and *in Situ* Raman spectroelectrochemistry of isotopically engineered graphene systems // Acc Chem Res. – 2015. – Vol. 48. – P. 111–118. https://doi.org/10.1021/ar500384p

14. Kavan L., Dunsch L. Spectroelectrochemistry of carbon nanostructures // ChemPhysChem. – 2007. – Vol. 8. – P. 974–998. https://doi.org/10.1002/cphc.200700081

15. Ferrari A.C., Meyer J.C., Scardaci V., Casiraghi C., Lazzeri M., Mauri F., Piscanec S., Jiang D., Novoselov K.S., Roth S., Geim A.K. Raman spectrum of graphene and graphene layers // Phys Rev Lett. – 2006. – Vol. 97. – Art. 187401. https://doi.org/10.1103/PhysRevLett.97.187401

16. Thomsen C., Reich S. Double resonant Raman scattering in graphite // Phys Rev Lett. – 2000. – Vol. 85. – P. 5214–5217. https://doi.org/10.1103/PhysRevLett.85.5214

17. Malard L.M., Pimenta M.A., Dresselhaus G., Dresselhaus M.S. Raman spectroscopy in graphene // Phys Rep. – 2009. – Vol. 473. – P. 51–87. https://doi.org/10.1016/j.physrep.2009.02.003

18. Ferrari A.C., Basko D.M. Raman spectroscopy as a versatile tool for studying the properties of graphene // Nat Nanotechnol. – 2013. – Vol. 8. – P. 235–246. https://doi.org/10.1038/nnano.2013.46

19. Ott A., Verzhbitskiy I.A., Clough J., Eckmann A., Georgiou T., Casiraghi C. Tunable D peak in gated graphene // Nano Res. – 2014. – Vol. 7. – P. 338–344. https://doi.org/10.1007/s12274-013-0399-2

20. Choi M., Son J., Choi H., Shin H., Lee S., Kim S., Lee S., Kim S., Lee K., Kim S.J., Hong B.H., Hong J., Yang I. *In-situ* Raman spectroscopy of current-carrying graphene microbridge // Journal of Raman Spectroscopy. – 2014. – Vol. 45. – P. 168–172. https://doi.org/10.1002/jrs.4442

21. Binder J., Urban J.M., Stepniewski R., Strupinski W., Wysmolek A. *In situ* Raman spectroscopy of the graphene/water interface of a solution-gated field-effect transistor: electron–phonon coupling and spectroelectrochemistry // Nanotechnology. – 2016. – Vol. 27. – Art. 045704. https://doi.org/10.1088/0957-4484/27/4/045704

22. Hiramatsu M., Hori M. Carbon nanowalls: Synthesis and emerging applications // Springer Vienna. – 2010. https://doi.org/10.1007/978-3-211-99718-5

23. Bohlooli F., Yamatogi A., Mori S. Manganese oxides/carbon nanowall nanocomposite electrode as an efficient non-enzymatic electrochemical sensor for hydrogen peroxide // Sens Biosensing Res. – 2021. – Vol. 31. – Art. 100392. https://doi.org/10.1016/j.sbsr.2020.100392

24. Tomatsu M., Hiramatsu M., Foord J.S., Kondo H., Ishikawa K., Sekine M., Takeda K., Hori M. Hydrogen peroxide sensor based on carbon nanowalls grown by plasma-enhanced chemical vapor deposition // Jpn J Appl Phys. – 2017. – Vol. 56. – Art. 06HF03. https://doi.org/10.7567/JJAP.56.06HF03

25. Bohlooli F., Anagri A., Mori S. Development of carbon-based metal free electrochemical sensor for hydrogen peroxide by surface modification of carbon nanowalls // Carbon N Y. – 2022. – Vol. 196. – P. 327–336. https://doi.org/10.1016/j.carbon.2022.05.002

26. Zhumadilov R.Ye., Yerlanuly Y., Kondo H., Nemkayeva R.R., Ramazanov T.S., Hori M., Gabdullin M.T. Hydrogen peroxide sensing with nitrogen-doped carbon nanowalls // Sens Biosensing Res. – 2024. – Vol. 43. – Art. 100614. https://doi.org/10.1016/j.sbsr.2023.100614

27. Markhabayeva A., Dupre R. ., Nemkayeva R. ., Nuraje N. Synthesis of hierarchical WO_3 microspheres for photoelectrochemical water splitting application // Physical Sciences and Technology. – 2023. – Vol. 10. – P. 33–39. https://doi.org/10.26577/phst.2023.v10.i2.04

28. Yerlanuly Y., Nemkayeva R. R., Zhumadilov R. Y., Gabdullin M. T. Investigation and evaluation of the morphology properties of carbon nanowalls based on fractal analysis and Minkowski functionals // Physical Sciences and Technology. – 2022. – Vol. 9. – P. 4–10. https://doi.org/10.26577/phst.2022.v9.i2.01

29. Myrzabekova M., Sarkar S., Baigarinova G., Guseinov N., Ilyin A. Obtaining and research of new composite materials polymer-graphene // Physical Sciences and Technology. – 2015. – Vol. 1. – P. 4–9. https://doi.org/10.26577/phst-2014-1-21

30. Yerlanuly Y., Christy D., Van Nong N., Kondo H., Alpysbayeva B., Nemkayeva R., Kadyr M., Ramazanov T., Gabdullin M., Batryshev D., Hori M. Synthesis of carbon nanowalls on the surface of nanoporous alumina membranes by RI-PECVD method // Appl Surf Sci. – 2020. – Vol. 523. – Art. 146533. https://doi.org/10.1016/j.apsusc.2020.146533

31. Xie Y., Huang Y., Zhang Y., Wu T., Liu S., Sun M., Lee B., Lin Z., Chen H., Dai P., Huang Z., Yang J., Shi C., Wu D., Huang L., Hua Y., Wang C., Sun S. Surface modification using heptafluorobutyric acid to produce highly stable Li metal anodes // Nat Commun. – 2023. – Vol. 14. – Art. 2883. https://doi.org/10.1038/s41467-023-38724-x

32. Fu Q., Wang X., Han J., Zhong J., Zhang T., Yao T., Xu C., Gao T., Xi S., Liang C., Xu L., Xu P., Song B. Phase-junction electrocatalysts towards enhanced hydrogen evolution reaction in alkaline media // Angewandte Chemie International Edition. – 2021. – Vol. 60. – P. 259–267. https://doi.org/10.1002/anie.202011318

33. Wang D., Liu C., Zhang Y., Wang Y., Wang Z., Ding D., Cui Y., Zhu X., Pan C., Lou Y., Li F., Zhu Y., Zhang Y. CO_2 electroreduction to formate at a partial current density up to 590 mA mg^{-1} via micrometer-scale lateral structuring of bismuth nanosheets // Small. – 2021. – Vol. 17. https://doi.org/10.1002/smll.202100602

34. Kurita S., Yoshimura A., Kawamoto H., Uchida T., Kojima K., Tachibana M., Molina-Morales P., Nakai H. Raman spectra of carbon nanowalls grown by plasma-enhanced chemical vapor deposition // J Appl Phys. – 2005. https://doi.org/10.1063/1.1900297

35. Davami K., Shaygan M., Kheirabi N., Zhao J., Kovalenko D.A., Rümmeli M.H., Opitz J., Cuniberti G., Lee J.-S., Meyyappan M. Synthesis and characterization of carbon nanowalls on different substrates by radio frequency plasma enhanced chemical vapor deposition // Carbon N Y. – 2014. – Vol. 72. – P. 372–380. https://doi.org/10.1016/j.carbon.2014.02.025

36. Liu R., Chi Y., Fang L., Tang Z., Yi X. Synthesis of carbon nanowall by plasma-enhanced chemical vapor deposition method // Journal of Nanoscience and Nanotechnology – 2014. – Vol. 14. – P. 1647-1657. https://doi.org/10.1166/jnn.2014.8905

37. Sun J., Sadd M., Edenborg P., Grönbeck H., Thiesen P.H., Xia Z., Quintano V., Qiu R., Matic A., Palermo V. Real-time imaging of Na^+ reversible intercalation in “Janus” graphene stacks for battery applications // Sci Adv. – 2021. – Vol. 7. https://doi.org/10.1126/sciadv.abf0812

38. Das A., Chakraborty B., Piscanec S., Pisana S., Sood A.K., Ferrari A.C. Phonon renormalization in doped bilayer graphene // Phys Rev B. – 2009. – Vol. 79. – Art. 155417. https://doi.org/10.1103/PhysRevB.79.155417

39. Das A., Pisana S., Chakraborty B., Piscanec S., Saha S.K., Waghmare U. V., Novoselov K.S., Krishnamurthy H.R., Geim A.K., Ferrari A.C., Sood A.K. Monitoring dopants by Raman scattering in an electrochemically top-gated graphene transistor // Nat Nanotechnol. – 2008. – Vol. 3. – P. 210–215. https://doi.org/10.1038/nnano.2008.67

40. Johra F.T., Lee J.-W., Jung W.-G. Facile and safe graphene preparation on solution based platform // Journal of Industrial and Engineering Chemistry. – 2014. – Vol. – 20. – P. 2883–2887. https://doi.org/10.1016/j.jiec.2013.11.022

41. Quezada-Renteria J.A., Ania C.O., Chazaro-Ruiz L.F., Rangel-Mendez J.R. Influence of protons on reduction degree and defect formation in electrochemically reduced graphene oxide // Carbon N Y. – 2019. – Vol. 149. – P. 722–732. https://doi.org/10.1016/j. carbon.2019.04.109

42. Ahn G., Ryu S. Reversible sulfuric acid doping of graphene probed by in-situ multi-wavelength Raman spectroscopy // Carbon N Y. – 2018. – Vol. 138. – P. 257–263. https://doi.org/10.1016/j.carbon.2018.05.065

43. Pinilla-Sánchez A., Chávez-Angel E., Murcia-López S., Carretero N.M., Palardonio S.M., Xiao P., Rueda-García D., Sotomayor Torres C.M., Gómez-Romero P., Martorell J., Ros, C. Controlling the electrochemical hydrogen generation and storage in graphene oxide by in-situ Raman spectroscopy // Carbon N Y. – 2022. – Vol. 200. – P. 227–235. https://doi.org/10.1016/j.carbon.2022.08.055

44. Hallam P.M., Banks C.E. Quantifying the electron transfer sites of graphene // Electrochem commun. – 2011. – Vol. 13. – P. 8–11. https://doi.org/10.1016/j.elecom.2010.10.030

45. Ambrosi A., Chua C.K., Bonanni A., Pumera M. Electrochemistry of Graphene and Related Materials // Chem Rev. – 2014. – Vol. 114. – P. 7150–7188. https://doi.org/10.1021/cr500023c

46. Kumar S., Baruah B., Kumar A. Tunable degree of oxidation through variation of H2O2 concentration and its effect on structural, optical and supercapacitive properties of graphene oxide powders synthesized using improved method // Mater Today Commun. – 2017. – Vol. 13. – P. 26–35. https://doi.org/10.1016/j.mtcomm.2017.08.007

47. Vimalanathan K., Scott J., Pan X., Luo X., Rahpeima S., Sun Q., Zou J., Bansal N., Prabawati E., Zhang W., Darwish N., Andersson M.R., Li Q., Raston C.L. Continuous flow fabrication of green graphene oxide in aqueous hydrogen peroxide // Nanoscale Adv. – 2022. – Vol. 4. – P. 3121–3130. https://doi.org/10.1039/D2NA00310D

48. Angizi S., Hong L., Huang X., Selvaganapathy P.R., Kruse P. Graphene versus concentrated aqueous electrolytes: the role of the electrochemical double layer in determining the screening length of an electrolyte // NPJ 2D Mater Appl. – 2023. – Vol. 7. – Art. 67. https://doi.org/10.1038/s41699-023-00431-y

49. Eigler S., Dotzer C., Hirsch A. Visualization of defect densities in reduced graphene oxide // Carbon N Y. – 2012. – Vol. 50. – P. 3666–3673. https://doi.org/10.1016/j.carbon.2012.03.039

Information about authors:

Zhumadilov Rakhymzhan, PhD ***i****s a Senior researcher at the Kazakh-British Technical University (Almaty, Kazakhstan), e-mail: rakimzhan@gmail.com*

Zhumadilov Rakhymzhan, PhD is a Senior researcher at the Kazakh-British Technical University (Almaty, Kazakhstan), e-mail: rakimzhan@gmail.com

Nemkayeva Renata is a Researcher at the Kazakh-British Technical University (Almaty, Kazakhstan), e-mail: quasisensus@mail.ru

Kondo Hiroki, PhD is a Professor at the Kyushu University (Fukuoka, Japan), e-mail: hkondo@ed.kyushu-u.ac.jp

Markhabayeva Aiymkul, PhD is a Senior researcher at the Kazakh-British Technical University (Almaty, Kazakhstan), e-mail: aiko_marx@mail.ru

Yerlanuly Yerassyl, PhD is a Senior researcher at the Kazakh-British Technical University (Almaty, Kazakhstan), e-mail: yerlanuly@ physics.kz

Gabdullin Maratbek., PhD is a Rector (Chairman of the Board) of the Kazakh-British Technical University (Almaty, Kazakhstan), e-mail: gabdullin@physics.kz

Hori Masaru, PhD is a Professor at the Nagoya University (Nagoya, Japan) e-mail: hori.masaru.g1@f.mail.nagoya-u.ac.jp

Supporting Information

In-situ Raman analysis of carbon nanowalls during electrochqmical measurement

Rakhymzhan Ye. Zhumadilov[1,2,3*], Bauyrzhan Ye. Zhumadilov[1,2], Renata R. Nemkayeva[1,2], Hiroki Kondo[4], Aiymkul A. Markhabayeva[1,2], Yerassyl Yerlanuly[1,2,3*], Maratbek T. Gabdullin[1,2,3] and Masaru Hori[5]

[1] *Kazakh-British Technical University, Almaty, Kazakhstan*
[2] *Al-Farabi Kazakh National University, Almaty, Kazakhstan*
[3] *Institute of Applied Science and Information Technologies, Almaty, Kazakhstan*
[4] *Kyushu University, Fukuoka, Japan*
[5] *Center for Low-temperature Plasma Sciences, Nagoya University, Nagoya, Japan*
[*] *e-mail*: rakimzhan@gmail.com, yerlanuly@physics.kz

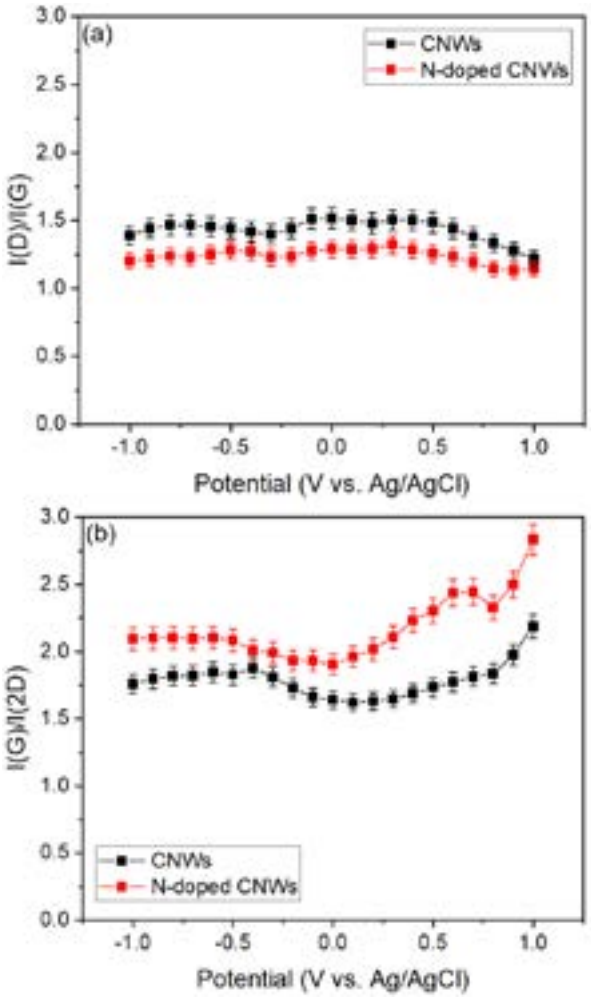

Figure S1 – (a) Dependences of the intensity ratio of the D and G peaks, and (b) dependence of the intensity ratio of the G and 2D peaks on the applied potential vs. Ag/AgCl.

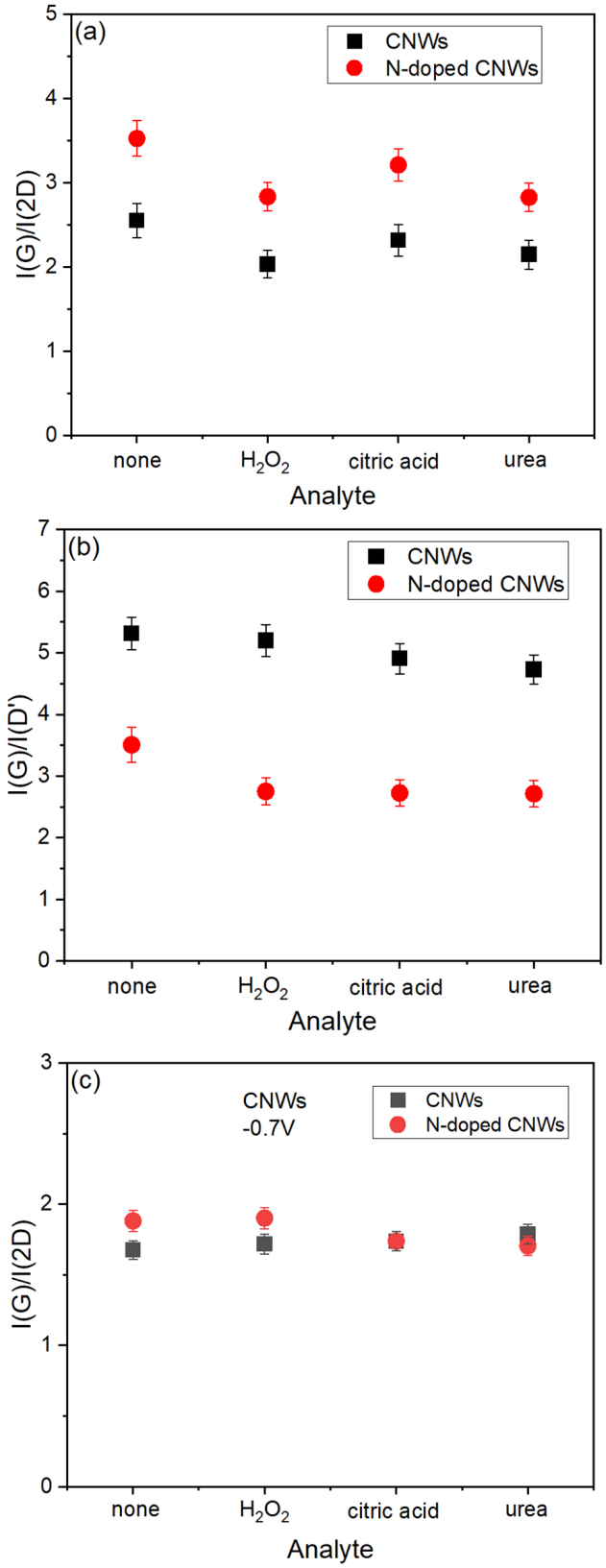

Figure S2 – (a) Dependences of the intensity ratio of the G and 2D peaks, (b) dependence of the intensity ratio of the G and D' peaks, and (c) dependence of the intensity ratio of the G and 2D peaks at -0.7V on the different analytes.